Continuous control of the nonlinearity phase for harmonic generations

Li, Guixin; Zhang, Shuang; Chen, Shumei; Pholchai, Nitipat; Reineke, Bernhard; Wong, Polis Wing Han; Yue Bun Pun, Edwin; Cheah, Kok-wai; Zentgraf, Thomas

DOI:
10.1038/nmat4267

Document Version
Peer reviewed version

Citation for published version (Harvard):
Li, G, Zhang, S, Chen, S, Pholchai, N, Reineke, B, Wong, PWH, Yue Bun Pun, E, Cheah, K & Zentgraf, T 2015, 'Continuous control of the nonlinearity phase for harmonic generations', *Nature Materials*, vol. 14, no. 6, pp. 607-612. https://doi.org/10.1038/nmat4267

Continuous control of nonlinearity phase for harmonic generations

Guixin Li[1,2†], Shumei Chen[1,2†], Nitipat Pholchai[3,4,5], Bernhard Reineke[3], Polis Wing Han Wong[6], Edwin Yue Bun Pun[6], Kok Wai Cheah[2]*, Thomas Zentgraf[3]*, and Shuang Zhang[1]*

[1]School of Physics & Astronomy, University of Birmingham, Birmingham, B15 2TT, UK

[2]Department of Physics, Hong Kong Baptist University, Kowloon Tong, Hong Kong

[3]Department of Physics, University of Paderborn, Warburger Straße 100, D-33098 Paderborn, Germany

[4]Department of Industrial Physics and Medical Instrumentation, King Mongkut's University of Technology North Bangkok, 1518 Pibulsongkram Road, Bangkok 10800, Thailand

[5]Lasers and Optics Research Group, King Mongkut's University of Technology North Bangkok, 1518 Pibulsongkram Road, Bangkok 10800, Thailand

[6]Department of Electronic Engineering, City University of Hong Kong, 83 Tat Chee Ave, Hong Kong

*email: kwcheah@hkbu.edu.hk; thomas.zentgraf@uni-paderborn.de; s.zhang@bham.ac.uk;

The capability of locally engineering the nonlinear optical properties of media is crucial in nonlinear optics. While poling is the most widely employed technique for achieving locally controlled nonlinearity, it only leads to a binary nonlinear state, which is equivalent to a discrete phase change of π in the nonlinear polarizability. Here, inspired by the concept of spin rotation coupling, we experimentally demonstrate nonlinear metasurfaces with homogeneous linear optical properties but spatially varying effective nonlinear polarizability with continuously controllable phase. The continuous phase control over the local nonlinearity is demonstrated for second and third harmonic generations by using nonlinear metasurfaces consisting of nanoantennas of C3 and C4 rotational symmetries, respectively. The continuous phase engineering of the effective nonlinear polarizability enables complete control over the propagation of harmonic generation signals. Therefore, it seamlessly combines the generation and manipulation of the harmonic waves, paving the way for highly compact nonlinear nanophotonic devices.

The local phase of the nonlinear polarizability determines how the generated nonlinear light in the material will interfere during its generation and propagation processes. In general one is interested in a constructive conversion of the fundamental to the nonlinear light while a wave is propagating through the material. However, the chromatic dispersion prevents from an efficient conversion due to the different propagation velocity of light for the different wavelengths. If the phase of the induced nonlinear material polarization can be controlled locally without modifying the linear properties such a mismatch can be avoided and the nonlinear process would be more efficient. Up to date there has been no demonstration of a material that allows continuous and arbitrary phase control for the local nonlinear polarizability. Such a nonlinear material would enable exact phase matching conditions for nonlinear optical processes, in contrast to the widely utilized quasi-phase matching scheme in which only the sign of the nonlinear polarizability can be manipulated[1-6]. It may remove additional undesired nonlinear processes which are introduced by the higher Fourier components of the nonlinear susceptibility in a periodically poled system. Metamaterials on the other hand provide a high degree of freedom for tailoring the local optical properties on a subwavelength scale. Nevertheless, they were mostly used for tailoring the linear optical properties.

The phase control over the nonlinear polarizability of the metamaterial is inspired by the concept of spin rotation coupling of light which has been utilized to control the wavefront of light in the linear regime[7-11]. This novel concept has been applied to the design of various types of functional metasurfaces[12-16]. These types of metasurfaces, which consist of plasmonic structures with subwavelength feature size (sometimes called "artificial atoms"), can be engineered to show rotation controlled local geometric phase shifts. This concept has been employed for flat lens imaging, generation of vortex beams, three-dimensional holography, and optical spin-orbital interaction[12-17]. Here we apply the concept of spin rotation coupling of light to the nonlinear regime leading to a nonlinear material polarization with arbitrarily controllable phase profile. For demonstration we show that this concept can be implemented by metasurfaces containing plasmonic antennas. However, we like to note that the concept of continuous phase control is universal and can be applied also to dielectric and bulk-like metamaterials.

We start by considering a single subwavelength plasmonic or dielectric nanostructure (resembling a dielectric dipole) embedded in an isotropic nonlinear medium (Fig. 1a). We will show that when excited by a circularly polarized fundamental beam, the phase of the nonlinear polarization of the artificial atom can be controlled geometrically by the orientation of the structure through a spin rotation coupling. For an incident fundamental beam with circular polarization state σ propagating along $+z$ direction, the electric field can be expressed as: $E^{\sigma} = E_0(e_x + i\sigma e_y)/\sqrt{2}$, where $\sigma = \pm 1$ represents the state of left- or right- handed circular polarization, respectively. The excitation of the nanostructures (e. g. the plasmonic nanorods) together with the nonlinear medium in close vicinity of the structure where the field can be strongly enhanced, locally forms an effective nonlinear dipole moment:

$$p_{\theta}^{n\omega} = \alpha_{\theta}(E^{\sigma})^n \qquad (1)$$

where α_{θ} is the n^{th} harmonic nonlinear polarizability tensor of the nanostructure with orientation angle of θ. We employ a coordinate rotation to analyze the dependence of the nonlinear dipole moment on the orientation angle of the nanostructure. In the local coordinate of the nanostructure (referred to as local frame) as shown in Fig. 1a where the local coordinate (x', y') axes are

rotated by an angle of θ with respect to the laboratory frame (x, y), the fundamental wave acquires a geometric phase due to the rotation spin coupling effect

$$E_L^{\sigma} = E^{\sigma} \mathrm{e}^{i\sigma\theta} \tag{2}$$

where the index 'L' denotes the nanostructure's local coordinate frame. The n^{th} harmonic nonlinear polarizability in the structure's local frame is simply $\alpha_0 = \alpha_{\theta}\big|_{\theta=0}$. Thus, the n^{th} harmonic nonlinear dipole moment in the local frame is given by

$$p_{\theta,L}^{n\omega} = \alpha_0 (E_L^{\sigma})^n = \alpha_0 (E^{\sigma})^n e^{in\sigma\theta} \tag{3}$$

The nonlinear dipole moment can be decomposed into two in-plane rotating dipoles (characterized by the circular polarization states σ and -σ) as

$$p_{\theta,L}^{n\omega} = p_{\theta,L,\sigma}^{n\omega} + p_{\theta,L,-\sigma}^{n\omega} \text{ with } p_{\theta,L,\sigma}^{n\omega}, p_{\theta,L,-\sigma}^{n\omega} \propto e^{in\sigma\theta} \tag{4}$$

After transforming back to the laboratory frame the two rotating dipole moments are given by

$$\begin{aligned} p_{\theta,\sigma}^{n\omega} &= p_{\theta,L,\sigma}^{n\omega} e^{-i\sigma\theta} \propto e^{(n-1)i\sigma\theta} \\ p_{\theta,-\sigma}^{n\omega} &= p_{\theta,L,-\sigma}^{n\omega} e^{i\sigma\theta} \propto e^{(n+1)i\sigma\theta} \end{aligned} \tag{5}$$

The nonlinear polarizabilities of the nanostructure can therefore be expressed as,

$$\begin{aligned} \alpha_{\theta,\sigma,\sigma}^{n\omega} &\propto e^{(n-1)i\sigma\theta} \\ \alpha_{\theta,-\sigma,\sigma}^{n\omega} &\propto e^{(n+1)i\sigma\theta} \end{aligned} \tag{6}$$

Thus, geometric phases of $(n-1)\sigma\theta$ or $(n+1)\sigma\theta$ are introduced to the nonlinear polarizabilities of the n^{th} harmonic generation with the same or the opposite circular polarization to that of the fundamental wave, respectively. According to the selection rules for harmonic generation of circular polarized fundamental waves, a single nanostructure with m-fold rotational symmetry only allows harmonic orders of $n = lm \pm 1$, where l is an integer, and the '+' and '-' sign correspond to harmonic generation of the same and opposite circular polarization, respectively[18-21]. The phases of the nonlinear polarizability for an incident fundamental wave of circular polarization, for various orders of harmonic generation and nanostructures of various rotational symmetries, are given in the Supplementary Materials (Table S1).

Hence for a nanorod structure with two-fold rotational symmetry ($C2$), THG signals with both the same and opposite circular polarizations as that of the fundamental wave can be generated. According to equation (6), they have a spin dependent phase of $2\sigma\theta$ and $4\sigma\theta$, respectively (Fig. 1b). On the other hand, a nanostructure with four-fold rotational symmetry ($C4$) does not allow a THG process for the same polarization state as the incident polarization. Hence, only a single THG signal, that of the opposite circular polarization, is generated with a geometric phase of $4\sigma\theta$ (Fig. 1c). Importantly, due to the local isotropic response of the C4 structure, both the polarization state and the propagation of the fundamental wave will not be affected when transmitting through a metamaterial consisting of such $C4$ nanostructures of arbitrary orientations. Thus, by assembling the $C4$ nanostructures with spatially varying orientations in a 3-D or 2-D lattice, a nonlinear metamaterial or metasurface can be formed which show homogeneous linear properties, but locally a well-defined nonlinear polarizability distribution for a circularly polarized fundamental wave.

We verify this concept of spin-rotation induced nonlinear phase by designing and fabricating three nonlinear binary phase gratings consisting of 2D arrays of plasmonic nanocrosses with a local $C4$ rotational symmetry (Fig. 2a-c). These binary nonlinear phase gratings can be easily used to characterize the relative phase of the nonlinear polarization between $C4$ nanostructures of different orientations. *Sample A* consists of nanocrosses of identical orientation along the entire lattice and a periodicity of $a = 400$ nm in both x- and y- axis directions, while *Sample B* and *Sample C* consist of supercells of nanocrosses with two different orientations and a superperiod of $P = 3.2$ μm (eight crosses per unit cell). The difference between the orientation angles of the two subsets of nanocrosses within a unit cell is $\pi/8$ and $\pi/4$ for *Sample B* and *C*, respectively. For the $C4$ structures, only THG of the opposite circular polarization as that of the incident fundamental beam is generated with a geometric phase of $4\sigma\theta$. Thus, the introduced nonlinear phase for *Sample B* and *Sample C* correspond to nonlinear phase gratings with phase difference of $\pi/2$ and π between the two subunits, respectively. For the binary nonlinear grating with period larger than the THG wavelength, the distribution of the nonlinear signal in different diffraction orders is solely determined by the phase difference between the two subsets. Thus, by experimentally measuring the ratio between the $0^{th}$and the 1^{st} order THG signals, we are able to verify the orientation controlled induced phase difference between the two subsets of nanocrosses within a unit cell in *Sample B* and *C*.

First, we coat a nonlinear active medium (PFO) on top of these three phase gratings to form a gold/PFO hybrid metasurface (see Methods Section). The linear optical properties of the hybrid phase gratings are characterized by using Fourier transformation infrared spectrometry. From the measured transmission spectra (Fig. 2d), we identify that the localized Plasmon resonance is around at wavelength: $\lambda \sim 1230$ nm for all three samples, and this also confirmed by the numerical simulation. Subsequently, we measured the THG signal from these three samples for a fundamental wavelength at the resonance dip to maximize the Plasmon enhanced nonlinear response from the samples. As shown previously[22-30], the combination of the strong field enhancement and large nonlinear polarizability of the plasmonic structures gives rise to a large nonlinear optical effect in such plasmonic system, making it easy to detect the generated nonlinear signal.

In the next step we illuminated the samples with short laser pulses at 1240 nm and measured the THG signal on a CCD camera. Our THG measurements with circular polarized incident light confirm the selection rules for the $C4$ symmetry structure as the THG signals with identical polarization states as the fundamental wave (RCP-RCP and LCP-LCP) are very weak for all three samples and therefore not visible in Fig. 2e. *Sample A*, with spatially homogenous orientation of the nanocrosses, only gives rise to a 0^{th} order THG. On the other hand, *Sample B* and *Sample C*, with their superlattice periodicity greater than the wavelength of the THG light, emit THG into the first diffraction orders. For *Sample B* where the phase difference between the third order nonlinearity of the two subsets of nanocrosses is $\pi/2$ the ratio between the 0^{th} order and the 1^{st} order THG signals is predicted to be ~ 2.4:1 (see Supplementary Materials Fig. S1 and the corresponding discussion). The measured ratio is around 2.8:1, which agrees very well with the theoretical prediction. The π phase difference between the nonlinear polarizabilities of the two subsets of the nanocrosses in *Sample C* is expected to result in a complete destructive interference for the 0^{th} order THG signal, which is confirmed by the measurement shown in the most right panel of Fig. 2e. The orientation angle dependent phase of nonlinearity is further confirmed by numerically calculating the contribution to the far field THG radiation from each

local point in the nonlinear medium, as shown in the Supplementary Materials Fig. S2 and S3. The simulation results provide an intuitive picture how the phase of the contribution varies with the orientation angle of the nanostructure for circularly polarized incident light.

Having confirmed the possibility for the geometric phase control of the nonlinear polarizabilities through variation of the orientation of the nanoantennas, we construct and fabricated two metasurfaces consisting of an array of plasmonic nanostructures with *C*2 (nanorod) and *C*4 (nanocross) rotational symmetry. For these samples, the orientation angle between the neighboring structures is linearly varied in order to obtain a linear phase gradient for the nonlinear polarization along the surface direction (Fig. 3a and Fig. 3b). Such phase gradient will lead to a tailored diffraction for the THG signal where the diffraction angle is determined by the phase gradient.

The linear diffraction of these metasurfaces for the fundamental beam is characterized at the wavelengths of 1.2 μm and 1.25 μm for the *C*2 and *C*4 metasurfaces, corresponding to their respective resonance wavelengths. The diffraction pattern, captured by an infrared CCD camera, is shown in Fig. 3c. For the *C*2 metasurface, the local anisotropy leads in the linear optical case to conversion between LCP and RCP, with a geometric phase given by twice the orientation angle of the nanorods. While the 0^{th} order has the same circular polarization as the incident beam, the beam with the opposite circular polarization is diffracted into the +1 or -1 order, depending on the incident circular polarization state. This diffraction effect arises from the spin dependent geometric phase in the linear regime, which has been investigated previously[12]. On the other hand, there is no diffraction observed for the *C*4 metasurface since locally the nanocrosses exhibit isotropic linear optical properties. Therefore, the *C*4 metasurface can be considered as a homogeneous optical surface in the linear regime, despite the spatial variation of the orientation angle along the surface.

THG measurements on the *C*2 and *C*4 metasurfaces for circularly polarized incident beams are subsequently carried out and the expected results for these two surfaces with the linear phase gradient are schematically illustrated in Fig. 4a. We observe that the THG signal with same and opposite polarization as that of the incident fundamental beam are generated on the *C*2 metasurface, while only the THG with opposite circular polarization is generated on the *C*4 sample. This again agrees with the selections rules of THG for nanostructures with different local symmetries. For the *C*2 sample (Fig. 4b), the THG signal is generated in four different diffraction orders, -2, -1, +1 and +2, which correspond to the incident/transmitted polarization of RCP/LCP, RCP/RCP, LCP/LCP and LCP/RCP, respectively. This can be explained by equation (5), where the nonlinear phase for the co-polarization and opposite polarization are $2\sigma\theta$ and $4\sigma\theta$, respectively, corresponding to the ±1 and ±2 diffraction orders for the *C*2 metasurface with a period of the orientation angle:$\Delta\theta = \pi$. On the other hand, for the *C*4 metasurface, only THG with polarization opposite to that of the incident beam is generated with the phase gradient of $4\sigma\theta$, which corresponds to the first diffraction orders for the *C*4 metasurfaces with period of $\Delta\theta = \pi/2$ for the orientation angle. For a circularly polarized dipole in the x-y plane, the emitted THG into a diffraction angle of φ in general contains both LCP and RCP components, with the ratio given by $(1-\cos\varphi)/(1+\cos\varphi)$. The periodicities of the nonlinear gratings in our work is 3.2 μm and the THG wavelength is 416 nm for the C2 metasurfaces. The diffraction angle φ of the first diffraction order for the THG signal is calculated as 7.5°, agreeing well with our measurement. As the diffraction angle is small, the THG signal is nearly a circularly polarized

beam, with the ellipticity given by $\psi = \tan^{-1}[(E_R - E_L)/(E_R + E_L)] = 0.991$. This is in agreement with our observation that the nonlinear signal is almost purely circularly polarized (Fig. 4b). The measurement nicely demonstrates the high potential for such spin rotation induced nonlinear phases in metamaterials: The *C*4 nonlinear nanostructures have orientation independent linear properties while the phase of the nonlinear polarization is orientation controlled by the building blocks of the material. Such properties are highly attractive for constructing nonlinear photonic devices such as nonlinear photonic crystals. It should be noted that pumping light needs to be at normal incidence, so that the rotational symmetry of the overall system is maintained. For light from oblique incidence, it is expected that nontrivial effects due to superposition of multipole contributions will affect both the linear and nonlinear properties[31].

As aforementioned, this concept of controlling the nonlinear phase is not confined to third harmonic generation, but can be applied to any harmonic order. As a confirmation of this claim we measured the second harmonic generation (SHG) for a metasurface consisting of C3 rotational symmetric structures for a linear phase gradient in the nonlinear polarization (Supplementary Material Fig. S4**)**. These measurements correspond to the same situation as shown in Fig. 4 but for SHG instead of THG and validates that the concept works also for other nonlinear processes.

Our work demonstrates that, through the spin rotation coupling of light with subwavelength sized nanostructures, a local continuous phase can be introduced into the nonlinear harmonic generation processes with metamaterials. We show that through this scheme we are able to continuously tune the phase of the nonlinear polarization in a metasurface consisting of nanocrosses with spatially varying orientations while preserving homogeneous linear optical properties. By controlling of local symmetry and global phase discontinuity, the spin dependent third harmonic diffraction from the nonlinear metasurface is experimentally demonstrated and agrees well with the theoretical predictions. Despite that we demonstrate a nonlinear metasurface with a phase gradient of the nonlinear polarizability along one direction, our metasurface can be readily designed and realized to have more complex phase profiles in the two in-plane directions, which is similar to the two dimensional (2-D) nonlinear photonic crystals first proposed by V. Berger[32] and experimentally realized by Broderick et al[33]. On the other hand, our metasurface goes beyond those previous works because of the continuous nonlinear phase profile, providing more powerful selection of the nonlinear reciprocal vectors involved in the nonlinear processes (e.g. by removing the higher frequency components unavoidable with the discrete poling steps). One key application of the 2-D nonlinear metasurfaces is the realization of nonlinear holograms, where a beam at fundamental wavelength can be converted to arbitrary beam profile at different wavelength. The continuous nonlinear phase profile of our metasurface would enable better control of the beam profile, meanwhile removing the issue of twin image generation that is intrinsic to a binary hologram. This approach for continuously controlling the nonlinearity can be potentially extended to three dimensional metamaterials made from low loss nonlinear dielectric nanostructures, for achieving custom defined local effective nonlinear susceptibilities, and introducing new freedoms in designing nonlinear materials for satisfying perfect phase matching conditions, nonlinear photonic crystals with arbitrary nonlinear phase profiles, and manipulation of nonlinear signals in integrated photonic circuits or in the free space.

Methods

Sample Fabrication. All the gold nanorods with thickness of 30 nm were fabricated on glass substrate using standard electron beam lithography (Crestec CABL-9510C) and followed by lift-off processes. All the gold metasurface devices were coated with 100-nm-thick poly(9,9-dioctylfluorence) (PFO) layer to form metal/organic hybrid nonlinear metasurfaces. Our previous studies have shown that the THG efficiency in the PFO/gold hybrid metasurface is much higher than that from PFO- or gold-only devices[21], indicating that the high nonlinear response is a combination of the field enhancement from the plasmonic structures and the large nonlinear coefficient of the PFO. In this work, the enhanced THG from the hybrid metasurface enables the easier detection of THG signals by using CCD camera.

THG Measurement. The diffraction of harmonic generations was measured using a femtosecond (fs) laser (repetition frequency: 80 MHz, pulse duration: ~ 200 fs) output from the optical parametric oscillator at wavelength which is close to the localized Plasmon resonance wavelengths of the nanostructures. The averaged power of the pumping laser is 30 mW. The laser with spot size of ~ 80 μm in diameter is normally incident on the metasurfaces after passing through an achromatic lens (f = 100 mm). The THG signals from gold/PFO metasurfaces are collected by an infinity-corrected objective lens (40x, NA = 0.6).The back-focal plane of the objective lens was imaged to a charge coupled device (CCD) camera after filtering the pumping laser using band-pass filters.

References

1. Armstrong, J. A., Bloembergen, N., Ducuing, J. & Pershan, P. S. Interactions between light waves in a nonlinear dielectric. *Phys. Rev*. **127**, 1918-1939 (1962).
2. Fejer, M. M., Magel, G. A., Jundt, D. H. & Byer, R. L. Quasi-phase-matched second harmonic generation: tuning and tolerances. *IEEE J. Quantum Electron*. **28**, 2631-2654 (1992).
3. Zhang, X., Lytle, A. L., Popmintchev, T., Zhou, X., Kapteyn, H. C., Murnane, M. M. & Cohen, O. Quasi-phase-matching and quantum-path control of high-harmonic generation using counterpropagating light. *Nat. Phys*. **3**, 270-275 (2007).
4. Ellenbogen, T., Voloch-Bloch, N., Ganany-Padowicz, A. & Arie, A. Nonlinear generation and manipulation of Airy beams. *Nat. Photon.* **3***,* 395-398(2009).
5. Xu, P. & Zhu, S. N. Quasi-phase-matching engineering of entangled photons. *AIP Advances* **2**, 041401(2012).
6. Zhu, S. N., Zhu, Y. Y., Qin, Y. Q., Wang, H. F., Ge, C. Z. & Ming, N. B. Harmonic generation in a Fibonacci optical superlattice of $LiTaO_3$. *Phys. Rev. Lett*. **78**, 2752-2755 (1997).
7. Berry, M. V. Quantal phase factors accompanying adiabatic changes. *Proc. R. Soc. London Ser. A* **392**, 45-57(1984).
8. Bhandari, R. Phase jumps in a QHQ phase shifter - some consequences. *Phy. Lett. A* **204**, 188-192 (1995).
9. Gori, F. Measuring stokes parameters by means of a polarization grating. *Opt. Lett.* **24**, 584-586 (1999).

10. Bomzon, Z., Kleiner, V. & Hasman, E. Pancharatnam-Berry phase in space-variant polarization state manipulations with subwavelength gratings. *Opt. Lett*. **26**, 1424 (2001).
11. Gorodetski, Y., Niv, A., Kleiner, V. & Hasman, E. Observation of the spin-based plasmonic effect in nanoscale structures. *Phys. Rev. Lett*. **101**, 043903 (2008).
12. Yu, N., Genevet, P., Kats, M. A., Aieta, F., Tetienne, J. P., Capasso, F. & Gaburro, Z. Light propagation with phase discontinuities: generalized laws of reflection and refraction. *Science* **334**, 333-337 (2011).
13. Ni, X., Emani, N. K., Kildishev, A., Boltasseva, V. A. & Shalaev, V. M. Broadband light bending with plasmonic nanoantennas. *Science* **335**, 427 (2012).
14. Chen, X., Huang, L. L., Mühlenbernd, H., Li, G. X., Bai, B., Tan, Q., Jin, G., Qiu, C. W., Zhang, S. & Zentgraf, T. Dual-polarity plasmonic metalens for visible light. *Nat. Commun*. **3**:1198 (2012).
15. Huang, L. L., Chen, X., Mühlenbernd, H., Zhang, H., Chen, S., Bai, B., Tan, Q., Jin, G., Cheah, K. W., Qiu, C. W., Li, J., Zentgraf, T. & Zhang, S. Three-dimensional optical holography using a plasmonic metasurface. *Nat. Commun*. **4**:2808 (2013).
16. Li, G. X., Kang, M., Chen, S. M., Zhang, S., Pun, E. Y. B., Cheah, K. W. & Li, J. Spin-enabled plasmonic metasurfaces for manipulating orbital angular momentum of light. *Nano Lett*. **13**, 4148-4151(2013).
17. Yin, X. B., Ye, Z. L., Rho, J., Wang, Y. & Zhang, X. Photonic spin Hall effect at metasurfaces. *Science* **339**, 1405-1407 (2013).
18. Burns, W. K. & Bloembergen, N. Third-harmonic generation in absorbing media of cubic or isotropic symmetry. *Phys. Rev. B* **4**, 3437-3450 (1971).
19. Bhagavantam, S. & Chandrasekhar, P. Harmonic generation and selection rules in nonlinear optics. *Proc. Indian Acad. Sci. A* **76**, 13-20 (1972).
20. Konishi, K., Higuchi, T., Li, J., Larsson, J., Ishii, S., & Kuwata-Gonokami, M., Polarization-controlled circular second-harmonic generation from metal hole arrays with threefold rotational symmetry, *Phys. Rev. Lett.*, **112**, 135502 (2014)
21. Chen, S. M., Li, G. X., Zeuner, F., Wong, W. H., Pun, E. Y. B., Cheah, Zentgraf, T., K. W. & Zhang, S. Symmetry selective third harmonic generation from plasmonic metacrystals. *Phys. Rev. Lett.* **113**, 033901 (2014).
22. Kauranen, M. & Zayats, A. V. Nonlinear plasmonics. *Nat. Photon.* **6**, 737-748 (2012).
23. Kujala, S., Canfield, B. K., Kauranen, M., Svirko, Y. & Turunen, J. Multipole interference in the second-harmonic optical radiation from gold nanoparticles. *Phys. Rev. Lett.* **98**, 167403 (2007).
24. Zhang, Y., Grady, N. K., Ayala-Orozco, C. & Halas, N. J. Three-dimensional nanostructures as highly efficient generators of second harmonic light. *Nano Lett.* **11**, 5519-5523 (2011).
25. Cai, W., Vasudev, A. P. & Brongersma, M. L. Electrically controlled nonlinear generation of light with plasmonics. *Science* **333**, 1720-1723 (2011).

26. Aouani, H., Cia, M. N., Rahman, M., Sidiropoulos, T. P. H., Hong, M., Oulton, R. F. & Maier, S. A. Multiresonant broadband optical antennas as efficient tunable nanosources of second harmonic light. *Nano Lett.* **12**, 4997-5002 (2012).
27. Utikal, T., Zentgraf, T., Paul, T., Rockstuhl, C., Lederer, F., Lippitz, M. & Giessen, H. Towards the origin of the nonlinear response in hybrid plasmonic systems. *Phys. Rev. Lett.* **106**, 133901 (2011).
28. Renger, J., Quidant, R., Van Hulst, N. & Novotny, L. Surface-enhanced nonlinear four-wave mixing. *Phys. Rev. Lett.* **104**, 046803 (2010).
29. Rose, A., Powell, D. A., Shadrivov, I. V., Smith, D. R. & Kivshar, Y. S. Circular dichroism of four-wave mixing in nonlinear metamaterials. *Phys. Rev. B* **88**, 195148 (2013).
30. Suchowski, H., O'Brien, K., Wong, Z. J., Salandrino, A., Yin, X. & Zhang, X. Phase mismatch-free nonlinear propagation in optical zero-index materials. *Science* **342**, 1223-1226 (2013).
31. Kruk, K. S., Decker, M., Staude, I., Schiecht, S., Greppmair, M., Neshev, D. N., & Kivshar, Y. S. Spin-polarized photon emission by resonant multipolar nanoantennas. *ACS Photonics*, **1**, 1218-1223 (2014).
32. Berger, V. Nonlinear photonic crystals. *Phys. Rev. Lett.* **81**, 4136-4139 (1998).
33. Broderick, N. G. R., Ross, G. W., Offerhaus, H. L., Richardson, D. J., Hanna, D. C. Hexagonally poled Lithium Niobate: a two-dimensional nonlinear photonic crystal. *Phys. Rev. Lett*. **84**, 4345-4348 (2000).

Acknowledgments

This work was partly supported by EPSRC. T. Z. and S. Z. acknowledge financial support by the European Commission under the Marie Curie Career Integration Program. N. P. and T. Z. acknowledge the financial support by the DFG Research Center TRR142 "Tailored nonlinear photonics". K. W. and E. P. would like to thank the support from Research Grant Council of Hong Kong under Projects HKUST2/CRF/11G and AoE/P-02/12. G. X. thank support from the High Performance Cluster Computing Centre, Hong Kong Baptist University.

Author contributions

SZ and TZ conceived the idea and experiment. BR, PWHW and EYBP fabricated the samples. GL, SC, NP, KWC and TZ performed the measurements. SC performed the simulation. GL, SZ and TZ wrote the paper. All authors participated in discussion.

Additional information

Competing financial interests

The authors declare no competing financial interests.

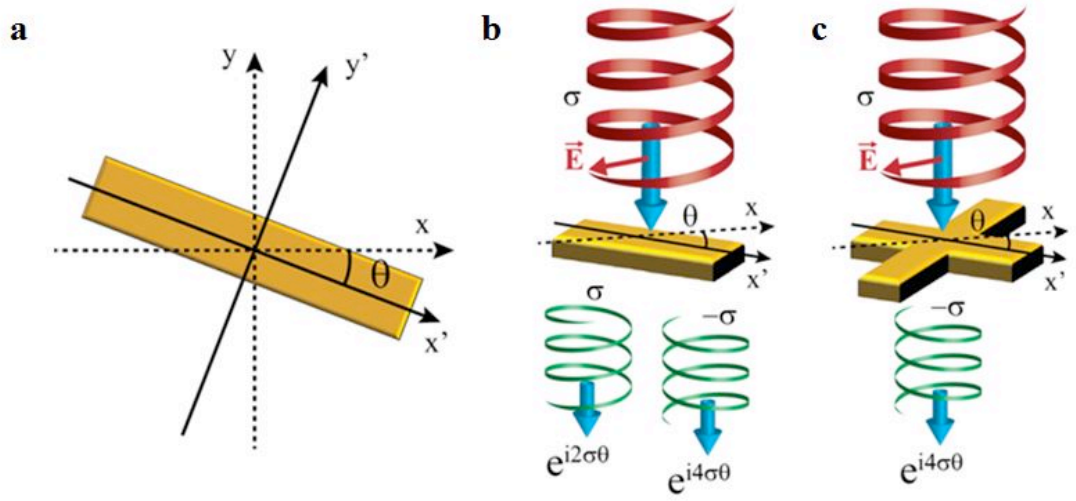

Figure 1| Illustration of geometric phase controlled nonlinear metamaterials. a, Rotating a nanostructure by an angle θ with respect to the laboratory frame will introduce a geometric phase. Hereby each nanostructure introduces a nonlinear geometric phase with a phase variation of (n-1)$\sigma\theta$ or (n+1)$\sigma\theta$ to the n^{th} harmonic generation for the same or the opposite circular polarization to that of the fundamental wave, respectively. **b**, For a *C*2 nanostructure, THG of both circular polarizations with phases of $2\sigma\theta$ and $4\sigma\theta$ are generated in the forward direction. **c**, For a *C*4 nanostructure, only THG with circular polarization opposite to that of fundamental wave is generated, which has a phase of $4\sigma\theta$.

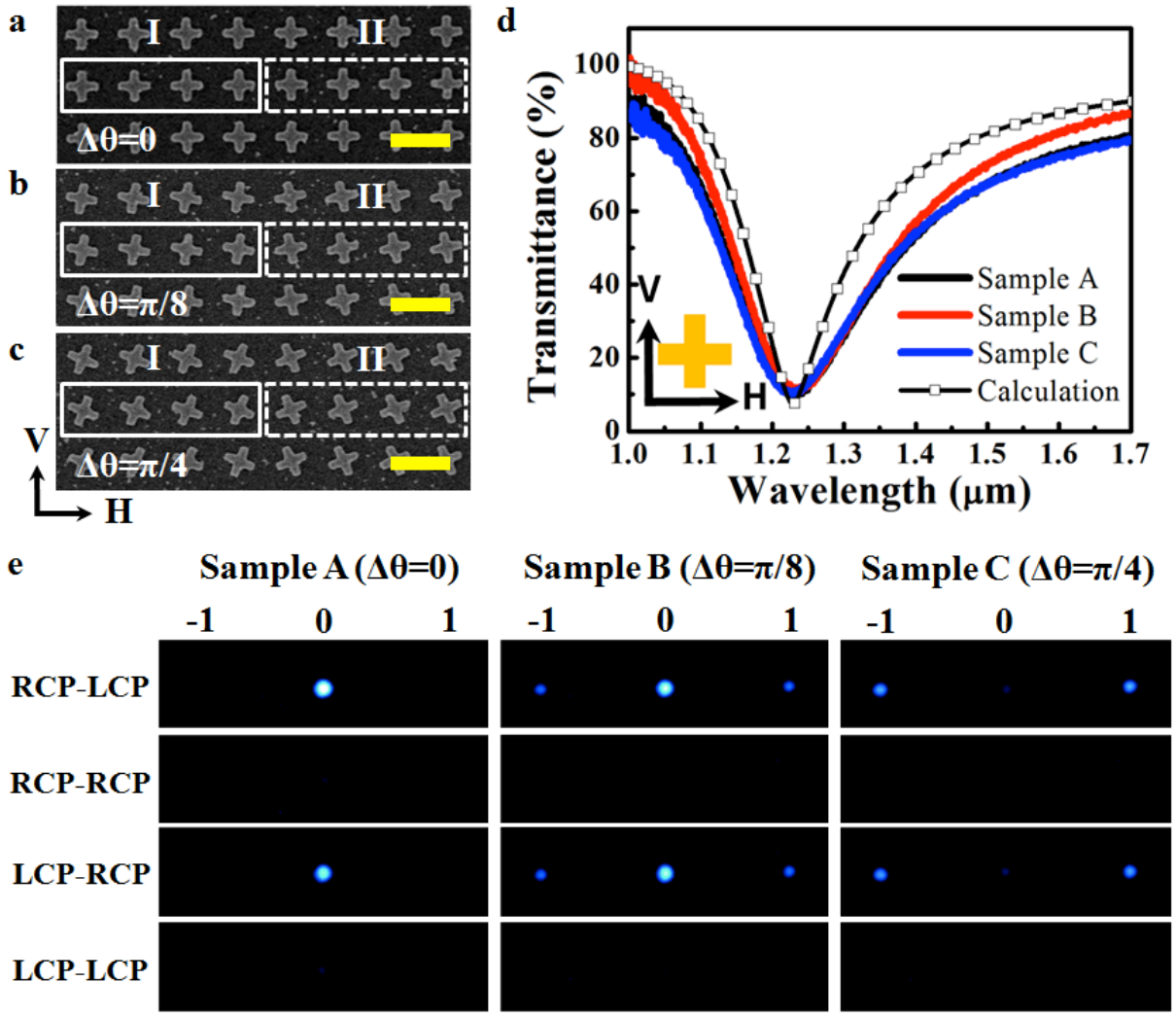

Figure 2| Experimental verification of the nonlinear phase with nonlinear phase gratings. **a-c**, Scanning electron microscopy images of *Sample A*, *B*, and *C* fabricated by electron beam lithography. The width and length of each gold nanorod are 50 nm and 240 nm, respectively. The lattice size for the three metasurfaces are a= 400 nm along x- (H) and y- (V) axis directions; thickness of gold layer is t = 30 nm. The scale bar shows 400 nm. **d**, Measured and simulated transmission spectra for the PFO coated hybrid metasurfaces showing the plasmonic resonance of the gold nanostructures for horizontal (H-) polarized illumination (see inset for the orientation of the axes). **e**, Measured diffraction pattern of THG signals from metasurfaces *A*, *B*, and *C*. The THG signals of the first and second rows correspond to right circularly polarized (RCP) pumping laser; the third and fourth rows corresponds to the left circularly polarized (LCP) pumping laser.

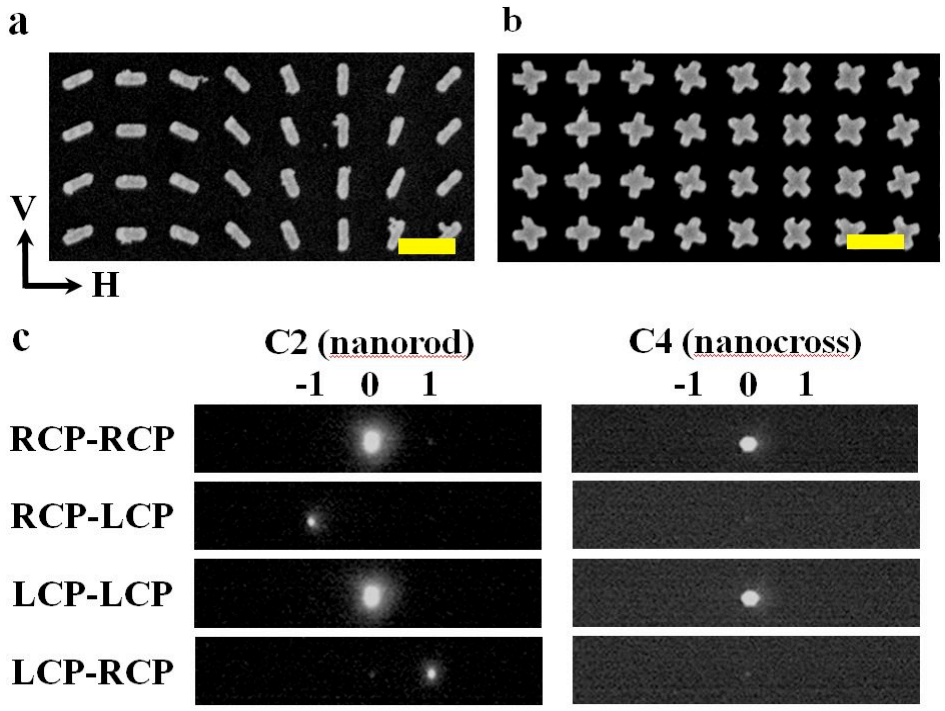

Figure 3| Diffraction of the fundamental wave on metasurfaces with linear phase gradients. **a**, **b**, Scanning electron microscopy images of metasurfaces consisting of *C*2 and *C*4 symmetry nanostructures. The lattice constant of the metasurfaces in both directions is a = 400 nm. Along the x direction (H) the nanostructures are rotated by an angle of $\pi/8$ for the *C*2 structures and $\pi/16$ for the *C*4 structures, respectively, resulting in the same superlattice period P=3.2 μm. scale bar: 400 nm. **c**, Measured diffraction pattern of the fundamental waves on the*C*2 (λ = 1250 nm) and the*C*4 (λ = 1200 nm) metasurfaces. The first and second rows were recorded using right circularly polarized (RCP) laser, while the third and fourth rows correspond to left circularly polarized (LCP) illumination.

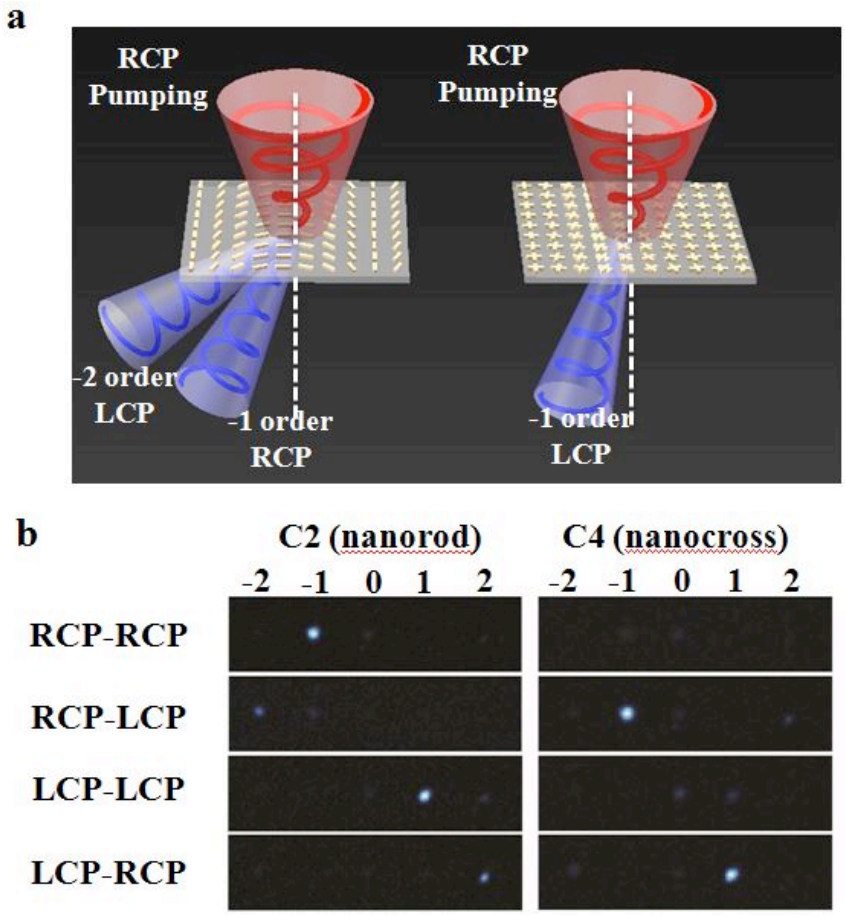

Figure 4| THG signals from metasurfaces with a phase gradient of the nonlinearity. a, Illustration of phase controlled diffractions of third harmonic generation (THG) for right circularly polarized (RCP) light at the fundamental frequency. The *C*2 symmetry metasurfaces diffract right- (RCP) and left- (LCP) circularly polarized THG signals to the first- and second-diffraction orders respectively; in comparison, the *C*4 symmetry metasurface only diffracts the opposite circularly polarized THG at first diffraction order direction. **b**, Measured diffraction pattern of the THG signals from the*C*2/PFO and *C*4/PFO metasurfaces for circular polarization states of the fundamental and the THG waves.